

# The differential magnification of high-redshift ultraluminous infrared galaxies

A. W. Blain

*Cavendish Laboratory, Madingley Road, Cambridge, CB3 0HE.  
Observatoire Midi-Pyrénées, 14 Avenue E. Belin, 31400 Toulouse, France.*

18 May 2018

## ABSTRACT

A class of extremely luminous high-redshift galaxies has recently been detected in unbiased submillimetre-wave surveys using the Submillimetre Common-User Bolometer Array (SCUBA) camera at the James Clerk Maxwell Telescope. Most of the luminosity of these galaxies is emitted from warm interstellar dust grains, and they could be the high-redshift counterparts of the low-redshift ultraluminous infrared galaxies (ULIRGs). Only one – SMM J02399–0136 – has yet been studied in detail. Three other very luminous high-redshift dusty galaxies with well determined spectral energy distributions in the mid-infrared waveband are known – IRAS F10214+4724, H1413+117 and APM 08279+5255. These were detected serendipitously rather than in unbiased surveys, and are all gravitationally lensed by a foreground galaxy. Two – H1413+117 and APM 08279+5255 – appear to emit a significantly greater fraction of their luminosity in the mid-infrared waveband, compared with both low-redshift ULIRGs and high-redshift submillimetre-selected galaxies. This can be explained by a systematically greater lensing magnification of hotter regions of the source compared with cooler regions: differential magnification. This effect can confuse the interpretation of the properties of distant ultraluminous galaxies that are lensed by intervening galaxies, but offers a possible way to investigate the temperature distribution of dust in their nuclei on scales of tens of pc.

**Key words:** galaxies: active – galaxies: individual: APM 08279+5255, H1413+117, IRAS F10214+4724 – cosmology: observations – gravitational lensing

## 1 INTRODUCTION

At wavelengths between about 10 and 1000  $\mu\text{m}$  the spectral energy distribution (SED) of a galaxy is dominated by the thermal emission from interstellar dust, which typically peaks at a wavelength of about 100  $\mu\text{m}$  (Sanders & Mirabel 1996). The dust is heated by absorbing the blue and ultraviolet light from young stars and active galactic nuclei (AGN). 100- $\mu\text{m}$  radiation from galaxies at redshifts less than about unity has been detected directly by the *IRAS* and *ISO* space-borne telescopes. The redshifted dust emission from more distant galaxies can be detected very efficiently at longer submillimetre wavelengths (Blain & Longair 1993a), as demonstrated by the discovery of SMM J02399–0136 at redshift  $z = 2.8$  (Ivison et al. 1998; Frayer et al. 1998) in a 850- $\mu\text{m}$  survey (Smail, Ivison & Blain 1997). Distant galaxies were also detected by *IRAS*, but only those with flux densities enhanced by gravitational lensing galaxies. Three such galaxies are known – IRAS F10214+4724 at  $z = 2.3$  (Rowan-Robinson et al. 1991), H1413+117 at  $z = 2.6$  (Barvainis et al. 1995) and APM 08279+5255 at  $z = 3.9$  (Irwin et

al. 1998; Lewis et al. 1998b; Downes et al. 1999). The SEDs of these high-redshift galaxies, and two well studied low-redshift ultraluminous infrared galaxies (ULIRGs) – Arp 220 and Markarian 231 (Klaas et al. 1997; Rigopoulou, Lawrence & Rowan-Robinson 1996; Soifer et al. 1999) – are shown in Fig. 1.

## 2 SPECTRAL ENERGY DISTRIBUTIONS

The difference in the slope of the mid-infrared SED of Arp 220 and Markarian 231 is interpreted as evidence for an active galactic nucleus (AGN) in the core of Markarian 231. Powerful ionizing radiation from an AGN would heat a very small fraction of the dust grains in the galaxy to high temperatures near the nucleus, increasing the flux density of the galaxy at short wavelengths and thus producing a shallower spectrum. There have been various attempts to interpret the mid-/far-infrared SEDs of galaxies using models of radiative transfer (Granato, Danese & Franceschini 1996; Green & Rowan-Robinson 1996). However, given that a power-law

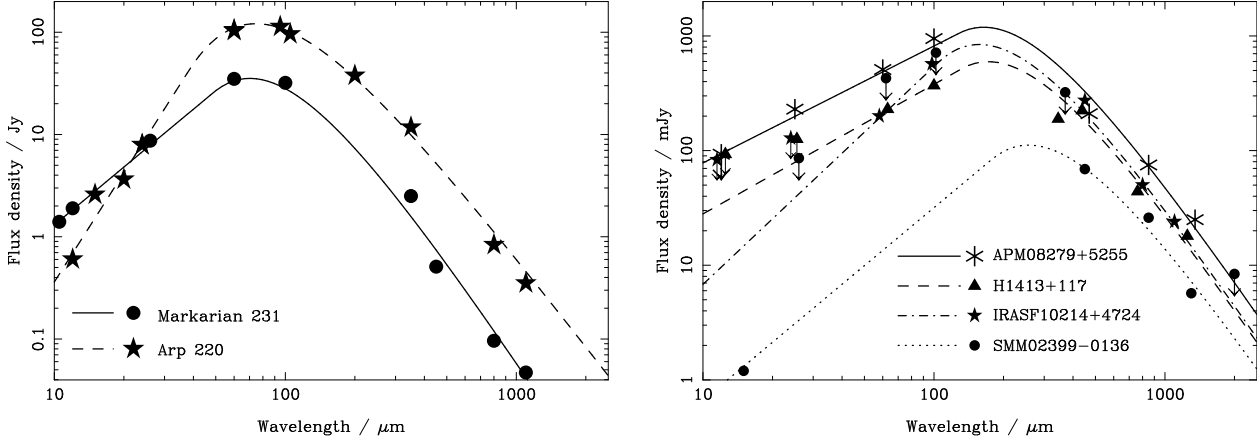


**Figure 1.** The SEDs of two low-redshift (left panel) and four high-redshift (right panel) ULIRGs. Note that the mid-infrared SEDs of the high-redshift galaxies APM08279+5255, H1413+117 and IRASF10214+4724 are probably modified by differential magnification. The SED models (lines) are described by a power-law,  $f_\nu \propto \nu^a$ , at short wavelengths and by a blackbody spectrum at temperature  $T_d$ , modified by a dust emissivity  $\epsilon_\nu \propto \nu^\beta$  with  $\beta \simeq 1$  at long wavelengths. The values of  $T_d$  and  $a$  in the models are listed in Table 1.

spectrum convincingly accounts for the limited mid-infrared data available, it is reasonable to avoid such modeling and to assume that the mass of emitting dust in the source at temperatures between  $T$  and  $T + dT$  is  $m_T(T) dT$ . Dust at each temperature can be associated with a  $\delta$ -function spectrum  $\delta(\nu - \nu_0)$ , in which  $\nu_0 \simeq (3 + \beta)kT/h$  (Blain & Longair 1993b).  $k$  and  $h$  are the Boltzmann and Planck constants respectively and  $\beta$  is the index in the function that describes the spectral emissivity of dust  $\epsilon_\nu \propto \nu^\beta$ ;  $\beta \simeq 1$ –1.5. The mid-infrared SED of a source at redshift  $z$  is

$$f_\nu \propto \int_{T_{\min}}^{T_{\max}} m_T(T) T^{4+\beta} \delta[\nu(1+z) - \nu_0] dT. \quad (1)$$

If  $m_T \propto T^\alpha$ , then the result is a power-law SED  $f_\nu \propto \nu^a$ , with a spectral index  $a = 4 + \alpha + \beta$ . For dust temperatures spanning a range from  $T_{\min} = 40$  K to  $T_{\max} = 2000$  K, this emission covers a range of wavelengths from about 90 to 1.8  $\mu\text{m}$ . The values of  $\alpha$  associated with the galaxies above are listed in Table 1.  $\alpha \simeq -6$  to  $-9$ , and so only a very small fraction of the dust in these galaxies is heated to high temperatures.

In the case that a significant fraction of dust heating in a galaxy is caused by an AGN, it would be reasonable to assume that the dust temperature would depend on the distance from the nucleus of the galaxy  $r$  as  $T_r(r) \propto r^\eta$ . A negative value of  $\eta$  would be expected, reflecting a higher dust temperature in the more intense radiation field closer to the AGN. If the mass of dust enclosed in the spherical shell between radii  $r$  and  $r + dr$  is  $m_r(r) dr$ , where  $m_r \propto r^\gamma$ , then the mid-infrared SED,

$$f_\nu \propto \int_{r_{\min}}^{r_{\max}} m_r(r) T_r(r)^{4+\beta} \delta[\nu(1+z) - \nu_0] dr, \quad (2)$$

again evaluates to a power law, with a spectral index  $a = 3 + \beta + (\gamma + 1)/\eta$ . Note that for a blackbody in equilibrium with an unobscured point source  $\eta = -0.5$ . In this case  $\gamma \simeq 2$  is required in order to represent the SEDs of Markarian 231 and SMM J02399–0136 in Fig. 1 – the distribution expected if the radial density of dust is uniform. A more reasonable value of  $\eta$  would be less than  $-0.5$ , reflecting the effects of

obscuration. This would imply that  $\gamma > 2$ , and thus that the density of emitting dust increases with increasing radius.

Two of the three high-redshift galaxies with *IRAS* detections – APM08279+5255 and H1413+117 – have a much flatter mid-infrared SED as compared with a typical low-redshift *IRAS* galaxy or SMM J02399–0136: see Fig. 1. SMM J02399–0136 lacks a detection by *IRAS*, but its mid-infrared SED is constrained by a 15- $\mu\text{m}$  *ISO* measurement of Metcalfe: see Ivison et al. (1998) for further details. Given the limited mid-infrared data for SMM J02399–0136, it is certainly possible that its mid-infrared spectral index could be more negative than the value of  $-1.7$  listed in Table 1. An additional high-redshift source, the brightest detected in a 850- $\mu\text{m}$  survey of the Hubble Deep Field (HDF; Hughes et al. 1998) with a flux density of 7 mJy, has a reported 15- $\mu\text{m}$  flux density limit of less than 23  $\mu\text{Jy}$ , indicating that its mid-infrared SED is steeper than that of SMM J02399–0136.

The slopes of these SEDs are not likely to be affected by contaminating sources that are picked up in the differently sized observing beams at each wavelength. The beam size of the 0.6-m telescopes used to determine the mid-infrared SEDs of these galaxies are about 5, 10, 25 and 40 arcsec at 12, 25, 60 and 100  $\mu\text{m}$  respectively, as compared with about 7 and 14 arcsec for the ground-based submillimetre-wave telescopes used at 450 and 850  $\mu\text{m}$  respectively. Any contamination from other sources nearby on the sky would thus be most significant at wavelengths of 60 and 100  $\mu\text{m}$ , and lead to an artificial steepening of the mid-infrared SED.

The shallow SEDs of APM08279+5255 and H1413+117 could be caused by an unusually large fraction of hot dust in these galaxies; however, from optical observations of their QSO emission both are known to be gravitationally lensed by magnification factors of at least several tens. A systematically greater magnification for hotter dust components would increase the flux density at shorter wavelengths and so flatten the spectrum (Eisenhardt et al. 1996; Lewis et al. 1998b). This situation would arise very naturally if the hotter dust clouds were smaller and more central, as in the AGN model described in equation (2). A similar effect can

**Table 1.** The redshift, restframe dust temperature, and mid-infrared spectral index  $a$  – where  $f_\nu \propto \nu^a$  – for the galaxies, the spectral energy distributions of which are plotted in Fig. 1. For comparison, the spectral index  $a \simeq -2.0$  to  $-2.5$  for samples of low-redshift *IRAS* galaxies, either those selected at a wavelength of  $25\ \mu\text{m}$  (Xu et al. 1998) or for the most luminous selected at  $60\ \mu\text{m}$  (Sanders & Mirabel 1996). The index  $\alpha$  that is required in the dust mass–temperature function  $m_T(T) \propto T^\alpha$ , in order to explain the mid-infrared spectral index is also listed for each source. Magnification factors of about 20, 35, 80 and 400 are required to make the 850-, 450-, 200- and  $50\text{-}\mu\text{m}$  flux densities of a  $z = 2.6$  counterpart of Markarian 231 equal to those of H1413+117.

Name	Redshift $z$	Restframe dust temperature $T_d$ / K	Mid-infrared spectral index $a$	Dust mass function index $\alpha$
Arp 220	0.02	50	-3.6	-8.6
Markarian 231	0.03	47	-1.9	-6.9
IRAS F10214+4724	2.3	76	-1.7	-6.0
H1413+117	2.6	75	-1.1	-6.7
SMM J02399–0136	2.8	53	-1.7	-6.1
APM08279+5255	3.9	107	-1.0	-6.7

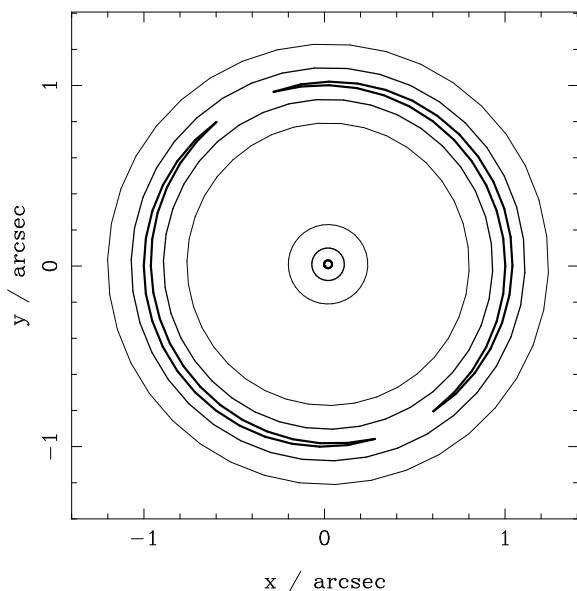


**Figure 2.** An illustration of the effect responsible for differential magnification, using a simple model of a lens as a SIS at  $z = 0.3$  with a one-dimensional velocity dispersion of  $150\ \text{km s}^{-1}$ . The lens is centred at the origin in the figure. The central circular contours mark isophotes that are 0.5, 2 and 5 kpc away from the centre of a source at  $z = 3$ , in order of decreasing line thickness. The source is centred  $0.022\ \text{arcsec}$  from the caustic of the lens at the origin. At  $z = 3$ ,  $1\ \text{arcsec}$  is equivalent to  $11.4\ \text{kpc}$ . The contours at radii of about  $1\ \text{arcsec}$  in the figure correspond to the mapped lensed images of the three source isophotes. The magnification for the region of the source enclosed within each isophote is 116, 45 and 18 respectively.

be produced by the microlensing effect of individual stars within the lensing galaxy (Lewis et al. 1998a).

For a large magnification to occur, a distant source must lie very close to a caustic curve of a gravitational lens. The magnification is formally infinite on such a curve, but an upper limit  $A_{\text{max}}$  is imposed to the magnification if the source has a finite size  $d$  (Peacock 1982). If the lensing galaxy can be modeled as a singular isothermal sphere (SIS), then  $A_{\text{max}} \propto d^{-1}$ . Assuming an SIS lens, the image geometry and magnifications expected in such a situa-

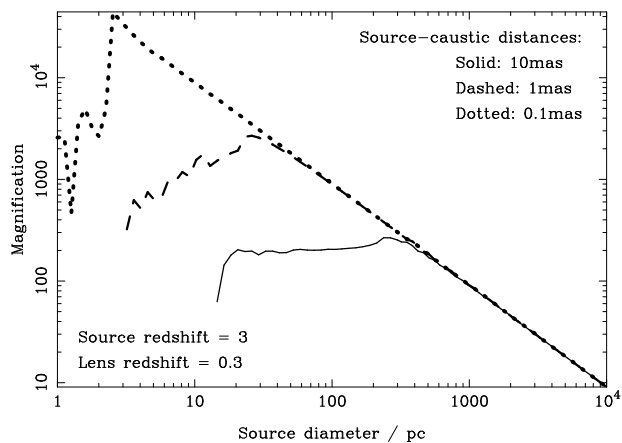


**Figure 3.** The magnification as a function of the source size for the SIS lens described in Fig. 2. The magnification is calculated assuming that the source is circular with a uniform surface brightness. The solid, dashed and dotted lines show the results for a source centred at points with three different offsets from the position of the point caustic of the SIS lens. The magnifications are large because an SIS lens is assumed. The argument in this paper depends on the relative magnification on different scales and not on the absolute magnification. For a similar plot derived for a detailed elliptical lens model of IRAS F10214+4724, see fig. 5 of Eisenhardt et al. (1996). The magnification curves depart from the uniform slope of  $-1$  on small scales when the caustic point no longer lies within the boundary of the circular source.

tion are illustrated in Figs 2 and 3. Eisenhardt et al. (1996) present more sophisticated lens models that account for the geometry of high-resolution images of IRAS F10214+4724. Ellipticity in the lens modifies the magnification–size relation to  $A_{\text{max}} \propto d^{-0.63}$  on scales between  $0.001$  and  $1\ \text{arcsec}$ . In general, a similar magnification–size relationship holds regardless of both the geometry of the source and whether one or more objects is responsible for producing the lensing effect (Kneib et al. 1998).

The diagnostic feature of such a situation is the production of multiple images of comparable brightness. This is clearly the case for both APM 08279+5255 (Lewis et al. 1998b) and H1413+117 (Kneib et al. 1998), but less so for IRAS F10214+4724, which has a more asymmetric arc-counterimage geometry. However, in the lens models

of both Broadhurst & Léhar (1995) and Eisenhardt et al. (1996), IRAS F10214+4724 lies very close to the tip of an astroid caustic, and so differential lensing would still be expected to flatten its mid-infrared SED. These references should be consulted for detailed lens models of these sources. The lens model if the most recently discovered source APM08279+5255 is poorly constrained because of the lack of high-resolution optical and near-infrared images at present.

If the smallest, hottest dust clouds that are closest to the AGN lie on the caustic that is responsible for the multiple images of the AGN (equation 2), then differential magnification of the hot regions compared with the cooler regions is likely to modify the SED in the mid-infrared waveband. The effect on the SED can be calculated by including a magnification factor of  $A_{\max}(r) \propto r^{-\mu}$  in the integrand of equation (2). For a SIS lens  $\mu = 1$ . By evaluating equation (2) in this case, a power-law SED with a spectral index  $a = 3 + \beta + (\gamma + 1 - \mu)/\eta$  is obtained. The spectral index is reduced by  $\Delta a = \mu/\eta$  compared with the value obtained in the absence of lensing. Note that the modification is independent of the value of  $\gamma$  and the form of  $m(r)$ . Following the same approach, but assuming an exponential decrease of  $T(r)$ ,  $\Delta a \simeq 1$ .

### 3 DISCUSSION

The mid-infrared SEDs of the high- and low-redshift AGNs SMM J02399–0136 and Markarian 231 have spectral indices  $a \simeq -1.8$ . Despite being lensed by a cluster of galaxies SMM J02399–0136 does not lie close to a caustic, and so is not magnified differentially. Markarian 231 is not lensed. The strongly lensed distant galaxies APM08279+5255 and H1413+117 have a spectral index  $a \simeq -1.1$ . This would indicate that  $\Delta a = \mu/\eta \simeq -0.7$ , and thus  $\eta \simeq -1.4$  or  $-0.9$ , depending on whether the lens is a SIS, with  $\mu = 1$ , or matches the model of Eisenhardt et al. (1996), with  $\mu = 0.6$ . Both spectral indices are considerably steeper than the un-screened blackbody value of  $-0.5$ . Given the very great opacity of interstellar dust to ionizing radiation, this is entirely reasonable. To match the observed SEDs, the corresponding values of  $\gamma$  of 7.3 and 4.0 are required, again indicating that most of the emitting dust is relatively cool/distant from the core.

#### IRAS F10214+4724

has a steeper mid-infrared SED, and a much smaller optical flux density than APM08279+5255 and H1413+117 (Lewis et al. 1998b). Its mid-infrared SED is more similar to those of Markarian 231 and SMM J02399–0136. These features could both be explained if the optical depth of dust extinction into the central regions of IRAS F10214+4724 were sufficiently large to obscure not only the AGN in the optical waveband, but also the hottest dust clouds at longer mid-infrared wavelengths. Alternatively, the intrinsic unmagnified SED of IRAS F10214+4724 could be steeper than those of APM08279+5255 and H1413+117, just as these two galaxies could have intrinsically flat mid-infrared SEDs.

Does the calculated value of  $\eta$  correspond to a plausible size for the emitting objects? The temperature of the inner face of the dust cloud exposed to the AGN cannot exceed about 2000 K, or else the dust would sublime. A 2000-K

blackbody would be in equilibrium with a  $10^{13}$ - $L_{\odot}$  point source at a distance of 0.6 parsec. If  $\eta = -1.4$ , then the dust temperature falls to 100, 50 and 30 K at distances of 5, 8 and 14 parsec respectively. If  $\eta = -0.9$ , then the corresponding distances are 9, 17 and 26 parsec. These values are all in agreement with observations of low-redshift ULIRGs, in which the emitting region is less than several hundreds of parsecs in extent (Downes & Solomon 1998). Most of the luminosity of the galaxy is emitted by cool dust on larger scales. The equivalent radius of a blackbody sphere emitting  $10^{13} L_{\odot}$  at 50 K is 950 pc, several times larger than the observed sizes of nearby ULIRGs (Downes & Solomon 1998; Sakamoto et al. 1999).

The caustic curves predicted by the lens models that describe IRAS F10214+4724 (Broadhurst & Léhar 1995) and H1413+117 (Kneib et al. 1998) are about 0.8 and 0.2 arcsec in size in the plane of the source, larger than the scale of a 200-pc high-redshift source. Hence, the whole emitting region of the source should be subject to differential magnification; a difference in magnification by a factor of about 100 would be obtained between a 200-pc outer radius and a 2-pc inner radius for an SIS lens.

If the far-infrared SED of a galaxy is modelled by a single-temperature dust spectrum, then differential magnification would be expected to increase the temperature for which the best fit was obtained. An increase in temperature by a factor of about 20 per cent would typically be expected for discrete data points at the wavelengths given in Fig. 1. This effect may account for at least part of the difference between the very high rest-frame dust temperature of about 107 K inferred for APM08279+5255 and the cooler dust temperatures inferred for nearby ULIRGs and SMM J02399–0136. If the redshift of a distant differentially magnified ULIRG were to be estimated from an observed SED, by fitting to a standard template, then the inferred redshift would be underestimated by a similar amount, up to 20 per cent.

The mid-infrared SEDs of distant galaxies that are known to be either unlensed or not to be subject to differential magnification are very uncertain. This is likely to remain true for some years, although the *Wide-Field Infrared Explorer (WIRE)* and *Space InfraRed Telescope Facility (SIRTF)* satellites will provide some valuable information. Operating at 12 and 25  $\mu\text{m}$ , *WIRE* will specifically probe the mid-infrared SED of distant galaxies. The effect of differential magnification discussed here could increase the number of lensed AGN detected in these bands by a factor of about 10; however, this number is still expected to be less than about 1 per cent of the size of the full *WIRE* catalogue.

AGN-powered ULIRGs are expected to have flatter mid-infrared SEDs than starburst-powered ULIRGs, even in the absence of differential magnification. Hence, any further flattening due to differential magnification should make it easier to distinguish AGN from starbursts in the subsample of lensed galaxies in the catalogue.

The flux density from the inner regions of an AGN can experience strong variation on short time-scales. On scales of several pc, the response of the hottest, smallest components of the mid-infrared dust emission spectrum should be comparable to the light-crossing time – about 1 yr. Over the lifetime of *SIRTF*, any such variations, amplified by differential magnification, should be detectable. In order to probe the

spatial structure and temperature distribution of dust in the inner regions of AGN directly, high-resolution mid-infrared imaging, and thus a space-borne mid-infrared interferometer, will be required (Mather et al. 1998a,b). Baselines of order 500 m at 20  $\mu\text{m}$  will be required to probe 10-pc scales in high-redshift galaxies.

The conditions in the central regions of AGN can already be probed using a variety of methods in other wavebands. Reverberation mapping – observing the transient response of line emission to a variable continuum source – is possible in the optical waveband (Bahcall, Kozlovsky & Salpeter 1972; Blandford & McKee 1982; Wandel 1997). Observations of water masers using very long baseline radio interferometry (Miyoshi et al. 1995) have revealed the structure of the accretion disk in NGC 4258. Modifications to the profiles of X-ray fluorescence lines due to strong gravity in the innermost regions of accretion disks have also been observed (Reynolds & Fabian 1997).

#### 4 CONCLUSIONS

(i) Distant lensed ULIRGs are likely to have their mid-infrared SEDs made more shallow by the effects of differential magnification. While observations of these sources must be exploited in order to investigate the nature of this class of galaxies, careful account must be taken of the uncertainties introduced by differential magnification. Recent submillimetre-selected samples are expected to be largely immune to this problem; their mid-infrared SEDs will be probed by the forthcoming *SIRTF* mission.

(ii) The SED of the longest known high-redshift ULIRG IRAS F10214+4724 is probably affected by differential magnification in the same way as those of APM 08279+5255 and H1413+117. However, it has a steeper mid-infrared SED. This could be due to either a steeper intrinsic SED, which is still flattened by differential magnification, or to a greater optical depth to dust extinction, which obscures the most central regions of the galaxy, even in the mid-infrared waveband.

(iii) The SEDs of a sample of lensed galaxies can be used to probe the conditions in the cores of distant dusty galaxies. A larger sample of these objects will be compiled by the *Planck Surveyor* satellite (Blain 1998). A direct test of the properties of dust in the central regions of high-redshift ULIRGs will require a space-borne interferometer such as *SPECS* (Mather et al. 1998a,b).

#### ACKNOWLEDGEMENTS

I thank Jean-Paul Kneib, Malcolm Longair, Priya Natarajan and an anonymous referee for their helpful comments on the manuscript, and PPARC and MENRT for support. This research has made use of the NASA/IPAC Extragalactic Database (NED) which is operated by the Jet Propulsion Laboratory, California Institute of Technology, under contract with the National Aeronautics and Space Administration.

#### REFERENCES

- Bahcall J. N., Kozlovsky B. Z., Salpeter E. E., 1972, *ApJ*, 171, 467  
 Barvainis R., Antonucci R., Hurt T., Coleman P., Reuter H.-P., 1995, *ApJ*, 451, L9  
 Blain A. W., 1998, *MNRAS*, 297, 511  
 Blain A. W., Longair M. S., 1993a, *MNRAS*, 264, 509  
 Blain A. W., Longair M. S., 1993b, *MNRAS*, 265, L21  
 Blandford R. D., McKee G. F., 1982, *ApJ*, 255, 419  
 Broadhurst T., Léhar J., 1995, *ApJ*, 459, L41  
 Downes D., Solomon P. M., 1998, *ApJ*, 507, 615  
 Downes D., Neri R., Wiklind T., Wilner D. J., Shaver P., 1999, *ApJL*, in press (astro-ph/9810111)  
 Eisenhardt P. R., Armus L., Hogg D. W., Soifer B. T., Neugebauer G., Werner M. W., 1996, *ApJ*, 461, 72  
 Frayer D. T., Ivison R. J., Scoville N. Z., Yun M. S., Evans A. S., Smail I., Blain A. W., Kneib J.-P., 1998, *ApJ*, 506, L7  
 Granato G. L., Danese L., Franceschini A., 1996, *ApJ*, 460, L11  
 Green S. M., Rowan-Robinson M., 1996, *MNRAS*, 279, 884  
 Hughes D. et al., 1998, *Nat*, 394, 241  
 Irwin M. J., Iwata R. A., Lewis G. F., Totten E. J., 1998, *ApJ*, 505, 529  
 Ivison R. J., Smail I., Le Borgne J.-F., Blain A. W., Kneib J.-P., Bézecourt J., Kerr T. H., Davies J. K., 1998, *MNRAS*, 298, 583  
 Klaas U., Haas M., Heinrichsen I., Schulz B., 1997, *A&A*, 325, L21  
 Kneib J.-P., Alloin D., Mellier Y., Guillotheau S., Barvainis R., Antonucci R., 1998, *A&A*, 329, 827  
 Lewis G. F., Irwin M. J., Hewett P. C., Foltz C. B., 1998a, *MNRAS*, 295, 573  
 Lewis G. F., Chapman S. C., Iwata R. A., Irwin M. J., Totten E. J., 1998b, *ApJ*, 1998b, 505, L1  
 Mather J. C. et al. 1998a, *BAAS*, 30(2), 861  
 Mather J. C., et al. 1998b, *SPECS* website <http://www.gsfc.nasa.gov/space/specs> (astro-ph/9812454)  
 Miyoshi M., Moran J., Hernstein J., Greenhill L., Nakai N., Diamond P., Inoue M., 1995, *Nat*, 373, 127  
 Peacock J. A., 1982, *MNRAS*, 199, 987  
 Reynolds C. S., Fabian A. C., 1997, *MNRAS*, 290, L1  
 Rigopoulou D., Lawrence A., Rowan-Robinson M., 1996, *MNRAS*, 278, 1049  
 Rowan-Robinson M. et al., 1991, *Nat*, 351, 719  
 Sakamoto K., Scoville N. Z., Yun M. S., Crosas M., Genzel R., Tacconi L. J., 1998, *ApJ*, in press (astro-ph/9810325)  
 Sanders D. B., Mirabel I. F., 1996, *ARA&A*, 34, 749  
 Smail I., Ivison R. J., Blain A. W., *ApJ*, 490, L5  
 Soifer B. T., Neugebauer G., Matthews K., Becklin E. E., Ressler M., Werner M. W., Weinberger A. J., Egami E. E., *ApJ*, in press (astro-ph/9810120)  
 Wandel A., 1997, *ApJ*, 490, L131  
 Xu C. et al. 1998, *ApJ*, 508, 576